Topotecan Combination Chemotherapy in Two New Rodent Models of Retinoblastoma

Nikia A. Laurie,[1] Jonathan K. Gray,[1] Jiakun Zhang,[1] Mark Leggas,[2] Mary Relling,[2] Merrill Egorin,[3] Clinton Stewart,[2] and Michael A. Dyer[1]

Abstract Chemotherapy combined with laser therapy and cryotherapy has improved the ocular salvage rate for children with bilateral retinoblastoma. However, children with late-stage disease often experience recurrence shortly after treatment. To improve the vision salvage rate in advanced bilateral retinoblastoma, we have developed and characterized two new rodent models of retinoblastoma for screening chemotherapeutic drug combinations. The first model is an orthotopic xenograft model in which green fluorescent protein – or luciferase-labeled human retinoblastoma cells are injected into the eyes of newborn rats. The second model uses a replication-incompetent retrovirus (LIA-E^{E1A}) encoding the *E1A* oncogene. Clonal, focal tumors arise from mouse retinal progenitor cells when LIA-E^{E1A} is injected into the eyes of newborn $p53^{-/-}$ mice. Using these two models combined with pharmacokinetic studies and cell culture experiments, we have tested the efficacy of topotecan combined with carboplatin and of topotecan combined with vincristine for the treatment of retinoblastoma. The combination of topotecan and carboplatin most effectively halted retinoblastoma progression in our rodent models and was superior to the current triple drug therapy using vincristine, carboplatin, and etoposide. Vincristine had the lowest LC_{50} in culture but did not reduce tumor growth in our preclinical retinoblastoma models. Taken together, these data suggest that topotecan may be a suitable replacement for etoposide in combination chemotherapy for the treatment of retinoblastoma.

Retinoblastoma is a childhood tumor of the retina that is usually detected during the first few years of life (1). In infants (younger than 1 year), retinoblastoma is the third most common form of cancer, next to neuroblastoma and leukemia (2, 3). Both heritable and sporadic forms of retinoblastoma result from inactivation of the retinoblastoma susceptibility gene, *RB1*. Children who inherit one defective copy of *RB1* are likely to develop bilateral, multifocal retinoblastoma as a result of inactivation of the second *RB1* allele (4). Sporadic retinoblastoma also results from *RB1* inactivation. However, due to the reduced probability of two spontaneous *RB1* mutations occurring in the same retinal cell during development, unilateral retinoblastoma tends to develop in children with the sporadic form of the disease (4, 5). Even with current anticancer therapy, metastatic retinoblastoma is often fatal (6). To minimize the risk of metastatic disease, patients with unilateral retinoblastoma undergo enucleation. Children with retinoblastoma in both eyes often undergo anticancer therapy to avoid bilateral enucleation and blindness. Chemotherapy combined with laser treatment and cryotherapy has improved the eye salvage rate for children with bilateral retinoblastoma and preserved vision for some patients (7). However, late-stage bilateral retinoblastoma remains difficult to treat with this approach (7). In addition, one of the drugs used to treat retinoblastoma worldwide (etoposide) is believed to be responsible for an increase in acute myeloblastic leukemia as a secondary malignancy (8). Alternative chemotherapeutic combinations have not been identified because there are too few patients for large-scale clinical trials. One approach that has recently been shown to be successful for another rare childhood cancer of the central nervous system (medulloblastoma) involves incorporating preclinical animal models to test new drugs before incorporation into clinical trials (9, 10).

There are currently two types of rodent models of retinoblastoma—xenograft and transgenic mouse models. The retinoblastoma xenograft model relies on injecting $>1 \times 10^6$ cultured human retinoblastoma cells into the flank of adult immunocompromised (severe combined immunodeficient) mice. This model fails to recapitulate the intraocular environment or developmental milieu that is present in children with retinoblastoma. Although a procedure for injecting human retinoblastoma cells into the eyes of adult severe combined immunodeficient mice has been reported (11, 12), this model has not been used extensively for testing new therapies nor does it recapitulate the developmental

Authors' Affiliations: Departments of [1]Developmental Neurobiology and [2]Pharmaceutical Sciences, St. Jude Children's Research Hospital, Memphis, Tennessee and [3]University of Pittsburgh Cancer Institute, Pittsburgh, Pennsylvania
Received 4/18/05; revised 6/28/05; accepted 7/15/05.

Grant support: National Eye Institute, National Cancer Institute, Pew Charitable Trust, Research to Prevent Blindness, and American Lebanese Syrian Associated Charities.

The costs of publication of this article were defrayed in part by the payment of page charges. This article must therefore be hereby marked *advertisement* in accordance with 18 U.S.C. Section 1734 solely to indicate this fact.

Requests for reprints: Michael A. Dyer, Department of Developmental Neurobiology, St. Jude Children's Research Hospital, Mail Stop 323, 332 North Lauderdale, Memphis, TN 38105-2794. Phone: 901-495-2257; Fax: 901-495-3143; E-mail: michael.dyer@stjude.org.

doi:10.1158/1078-0432.CCR-05-0849

environment of human retinoblastoma. The existing transgenic mouse models of retinoblastoma rely on the broad ectopic expression of the SV40 T oncogene to lead to massive hyperproliferation (13). The limitation of this transgenic mouse model is the lack of focal, clonal tumors. Large regions of the retina are genetically altered, predisposing the cells to undergo malignant transformation. However, retinoblastomas arise from one individual cell leading to a few tumor foci in children. Recently, the first knockout mouse model of retinoblastoma was generated by conditionally deleting *RB* in retinal progenitor cells of a *p107*-deficient mouse (14). When *p53* was simultaneously inactivated in *RB*, *p107*-deficient retinal progenitor cells, a more aggressive form of retinoblastoma was observed that is similar to the human disease (14). Two other laboratories have generated similar models of retinoblastoma using Cre-transgenic lines with broad expression in the peripheral retina (15) or developing central nervous system (16).

We have focused on the developmental environment and focal origins of retinoblastoma in developing two new rodent models for testing the efficacy of combination chemotherapy. In our xenograft model, we injected 1,000 green fluorescent protein (GFP)– or luciferase-labeled human retinoblastoma cells into the eyes of newborn rats to create a developmentally appropriate, orthotopic xenograft model of childhood retinoblastoma. In our genetic model, we injected a replication-incompetent retrovirus encoding the *E1A* 13S oncogene into newborn p53-deficient mice to induce clonal retinal tumors that arise from one to five individual foci. Importantly, these cells spread laterally through the retinal vasculature, a key feature of many types of cancer and particularly important for testing angiostatic anticancer therapies.

One of the most widely used chemotherapeutic protocols for the treatment of retinoblastoma includes a triple therapy of carboplatin, vincristine, and etoposide. Even when combined with focal therapies, the triple drug combination is ineffective in as many as 40% of bilateral retinoblastoma patients (7). Moreover, etoposide has been found to increase the incidence of secondary malignancies likely due to DNA damage caused by this topoisomerase II inhibitor. In contrast, topotecan, a topoisomerase I inhibitor, does not cause secondary malignancies and has been used successfully to treat other childhood cancers of the nervous system (17–22). Our data show that the combination of topotecan and carboplatin is the most effective treatment for retinoblastoma in our animal models. Although vincristine is an effective antitumor drug in culture and penetrates the blood-ocular barrier, the slow kinetics of action or intraocular instability may reduce efficacy *in vivo*. Taken together, our cell culture studies, ocular pharmacokinetics, and studies with two new preclinical models of retinoblastoma suggest that topotecan/carboplatin combination chemotherapy may be an effective substitute for etoposide/vincristine/carboplatin triple drug therapy.

Materials and Methods

Cell culture. Y79 and Weri1 cells were obtained from the American Type Culture Collection (Manassas, VA) and maintained in culture in RPMI with 10% FCS (23). Stable lines expressing GFP were generated by transfecting pTET-1[4] into Y79 and Weri1 cells by using TransFast (Promega, Madison, WI); clones were isolated in the presence of hygromycin. Y79-LUC cells were generously provided by Dr. Andrew Davidoff (St. Jude Children's Research Hospital, Memphis, TN). To measure live cells, 0.5 μg/mL calcein was used; to measure dead cells, 4 μmol/L ethidium bromide was used.

Immunolabeling and terminal deoxynucleotidyl transferase–mediated dUTP nick end labeling and bromodeoxyuridine assays. Y79 and Weri1 retinoblastoma cells were immunolabeled as described previously for dissociated mouse retinae (24–26). For *in vivo* studies, bromodeoxyuridine (BrdU; 100 mg/kg body weight) was given via tail vein injection. BrdU and terminal deoxynucleotidyl transferase–mediated dUTP nick end labeling (TUNEL) assays were carried out as described previously (24–26). Detailed protocols are available at http://www.stjude.org/dyer.

Fluorescent-activated cell sorting. DNA content was analyzed by dissociating tumors with trypsin (24–26) and sorting cells by fluorescent-activated cell sorting. Cells were washed with PBS and resuspended in a solution containing 0.05 mg/mL propidium iodide, 0.1% sodium citrate, and 0.1% Triton X-100. Samples were then treated with RNase, filtered through a 40-μm nylon mesh, and analyzed on a FACScan (Becton Dickinson, Franklin Lakes, NJ).

Determination of maximum tolerated dose. To determine the maximum tolerated dose (MTD) of vincristine, topotecan, etoposide, and carboplatin individually and in combination, cohorts of 15 P14 rats were given a single dose of each drug by tail vein injection or i.p. injection. The animals were monitored daily for physical appearance and weight loss. Animals that were moribund or lost 20% of their original body weight were euthanized. The MTD was the dose at which 100% of the animals tolerated systemic exposure for 2 weeks. The MTDs for P14 rats are listed below under pharmacology. p53-deficient mice received much lower doses of each drug than the MTD to more accurately mimic the dose and schedule children receive. Weight was monitored throughout the trial, and there was no significant weight loss or other visible signs of distress for any of the drug combinations tested in this study.

Pharmacology. Two-week-old rats were treated with topotecan (Hycamtin; GlaxoSmithKline, Research Triangle Park, NC) at a MTD of 2 mg/kg body weight, carboplatin (Paraplatin; Bristol-Myers Squibb, New York, NY) at a MTD of 70 mg/kg, vincristine (Mayne Pharma, Inc., Paramus, NJ) at a MTD of 0.5 mg/kg, and etoposide (Bedford Laboratories, Inc., Bedford, OH) at a MTD of 10 mg/kg; all agents were given via tail vein injection. Topotecan was measured by high-performance liquid chromatography as described (18). Atomic absorption spectrometry of ultrafiltered and nonfiltered samples was used to measure platinum concentrations (27). Liquid scintillation was used to measure concentrations of [^{3}H]vincristine (70-90 Ci/mmol; Perkin-Elmer, Wellesley, MA). Plasma, vitreous, and retinal lysates from P14 rats treated with etoposide were mixed with absorbic acid and analyzed by high-performance liquid chromatography as described (28). Six-week-old mice received topotecan (0.1 mg/kg), carboplatin (18 mg/kg), and vincristine (0.01 mg/kg) at doses and schedules comparable with that used to treat children with brain tumors (29). Specifically, they received daily × 5 topotecan and then once weekly carboplatin or vincristine. This was repeated on week 2 with no topotecan treatment on week 3. The 3-week cycle was repeated thrice, and animals were sacrificed and tumors were analyzed. Etoposide was given once weekly along with the other drugs for 8 weeks.

Animals, tissues, and retroviruses. The $p53^{-/-}$ mice were obtained from the MMCR at the National Cancer Institute. All mice were crossed to C57BL/6 mice purchased from Charles River Laboratories (Wilmington, MA). Timed-pregnant Sprague-Dawley rats were also purchased from Charles River Laboratories. Retroviral procedures have been described elsewhere (14, 24, 30, 31).

[4] M.A. Dyer, unpublished data.

Microscopy and tumor reconstruction. Bright-field and single-cell fluorescent images were obtained using a Zeiss Axioplan 2 fluorescent microscope with the Zeiss AxioCam digital camera. Fluorescent images of tissue sections were obtained using a Leica TCSNT confocal microscope. Tumor reconstruction was carried out using BioQuant 5.0 software.

Xenogen imaging of Y79-LUC cells **in vivo.** Cell injections were done as described for Y79-GFP cells. To monitor the luciferase activity, rats received an i.p. injection of avertin followed by an i.p. injection of Luciferin (Xenogen, Inc., Alameda, CA) according to the manufacturer's instructions. Five minutes later, the eyes were imaged using the Xenogen luciferase imaging system.

Viable cell calculation following drug treatment. Following drug treatment, the total number of cells (N) were scored and this was followed by calcein and ethidium bromide staining to determine the proportion (calcein / calcein + ethidium bromide) of those cells that were metabolically active (M). The proportion of cells that had initiated apoptosis (T) was determined by a TUNEL assay. In a separate experiment, we determined that 90.7% of TUNEL-labeled cells were also identified as nonmetabolically active by ethidium bromide staining. Therefore, $1 - 0.907T$ is the proportion of nonviable cells that had initiated apoptosis but were not yet detected by other means. All of these data were combined to obtain the number of viable cells in the following equation: number of viable cells = $N \times M \times (1 - 0.907T)$.

The proportion of viable cells is the ratio of the number of viable cells for the treated sample over the untreated sample. All of the cell culture experiments were carried out twice in triplicate totaling over 750 individual cultures. Each individual culture was then scored manually in duplicate (~ 500 cells each) for viability (calcein/ethidium bromide), proliferation (BrdUrd), apoptosis (TUNEL), and cell number (see Materials and Methods) totaling over 1 million cells scored to generate the data shown in Figs. 1 and 2.

Results

Effects of topotecan, carboplatin, vincristine, and etoposide on cultured retinoblastoma cells. As a first step toward analyzing the efficacy of topotecan for the treatment of retinoblastoma, we treated Y79 and Weri1 cultured retinoblastoma cells with topotecan and directly compared the results with data obtained using etoposide, vincristine, and carboplatin treatment individually. The Y79 and Weri1 cells were treated with each drug or drug combination just as they were entering their optimal growth phase (0.3×10^6-0.4×10^6 cells/mL; Fig. 1A). Each cell line was exposed to six different concentrations (1 nmol/L-100 μmol/L) of each drug for 8 hours, and 72 hours later, the total cell number was determined for each treatment in triplicate. To determine the proportion of cells that were viable following drug exposure, each sample was stained with calcein, which labels cells that are metabolically active, and ethidium bromide, which labels the nuclei of nonviable cells (Fig. 1B). The proportion of cells that had initiated apoptosis as a result of drug exposure was quantitated using a TUNEL assay for each sample (Fig. 1B). To study the effects on proliferation, BrdU was added to the culture medium 1 hour before analysis and the proportion of BrdU-positive cells was quantitated for each drug at each concentration in triplicate (Fig. 1B). All experiments were done in duplicate. These data were combined to generate an overall proportion of viable cells at each drug concentration (see Materials and Methods for calculations; Fig. 1C).

Topotecan is a topoisomerase I inhibitor that induces single-strand breaks in the DNA. The LC_{50} for topotecan was 30 nmol/L for Y79 cells and 19 nmol/L for Weri1 cells (Fig. 1C; data not shown). Vincristine blocks M phase by blocking microtubule formation (32) and has a potent antiproliferative effect on tumor cells with high mitotic indices similar to retinoblastoma. The LC_{50} of vincristine was 5 nmol/L for Y79 cells and 3 nmol/L for Weri1 cells (Fig. 1C; data not shown). Like topotecan, carboplatin also induces DNA damage, but rather than DNA breaks, it forms platinum-DNA adducts that can block DNA replication and transcription (33). The LC_{50} of carboplatin was 4 μmol/L for Y79 cells and 5 μmol/L for Weri1 cells (Fig. 1C; data not shown). Etoposide is a topoisomerase II inhibitor that leads to double-strand DNA breaks and it is included in these studies because it is a component of the current triple drug (etoposide, carboplatin, and vincristine) chemotherapy protocol for the treatment of retinoblastoma. The LC_{50} of etoposide was 1.8 μmol/L for Y79 and 0.2 μmol/L for Weri1 cells (Fig. 1D; data not shown).

Combination chemotherapy is often more effective than single drug therapy and this is one of the reasons that vincristine and carboplatin are combined with etoposide in the current triple drug therapy for retinoblastoma. The combination of vincristine and carboplatin with etoposide results in an additive reduction in the proportion of viable retinoblastoma cells compared with etoposide exposure alone (Fig. 1D). At carboplatin concentrations of 2 nmol/L to 200 μmol/L, the topotecan and carboplatin combination more effectively reduced cell viability and proliferation than either drug alone (Fig. 1D; data not shown). This effect was additive. Similarly, at vincristine concentrations of 1 to 10 nmol/L, the topotecan and vincristine combination was more effective at reducing cell viability and proliferation than either drug alone (Fig. 1D; data not shown). Concentrations of vincristine higher than 10 nmol/L showed no added benefit in combination treatment in these culture experiments.

Analysis of the minimum time of exposure for topotecan, vincristine, carboplatin, and etoposide. The cell culture experiments described above allowed us to directly compare the activity of etoposide, vincristine, carboplatin, and topotecan against retinoblastoma cells using their LC_{50} calculations. However, the drug with the lowest LC_{50} value may not necessarily be the most effective drug *in vivo*. For example, a drug with a relatively high LC_{50} may exhibit greater efficacy *in vivo* than a drug with a low LC_{50} if it is a faster-acting drug. That is, if the intraocular concentration of a drug reaches sufficient levels to induce a significant reduction in cell viability for only a short amount of time, then it must be a fast-acting drug to achieve any antitumor efficacy *in vivo*. To determine the minimum time of exposure to achieve the maximum reduction in the proportion of viable cells, we exposed Weri1 and Y79 cell cultures to each drug at their LC_{50} concentrations for different amounts of time ranging from 5 minutes to 8 hours (Fig. 2A). As with the previous experiments (see Fig. 1), the cell number, cell viability (calcein/ethidium bromide), apoptosis (TUNEL), and proliferation (BrdU) were measured at each time point for each drug. As little as 15 minutes of exposure to topotecan or carboplatin was sufficient to achieve the maximum reduction in cell survival and proliferation (Fig. 2A). The effects of vincristine and etoposide were much slower with a maximum decrease in viability at 4 and 6 hours, respectively (Fig. 2A). Fluorescent-activated cell sorting analysis of these samples

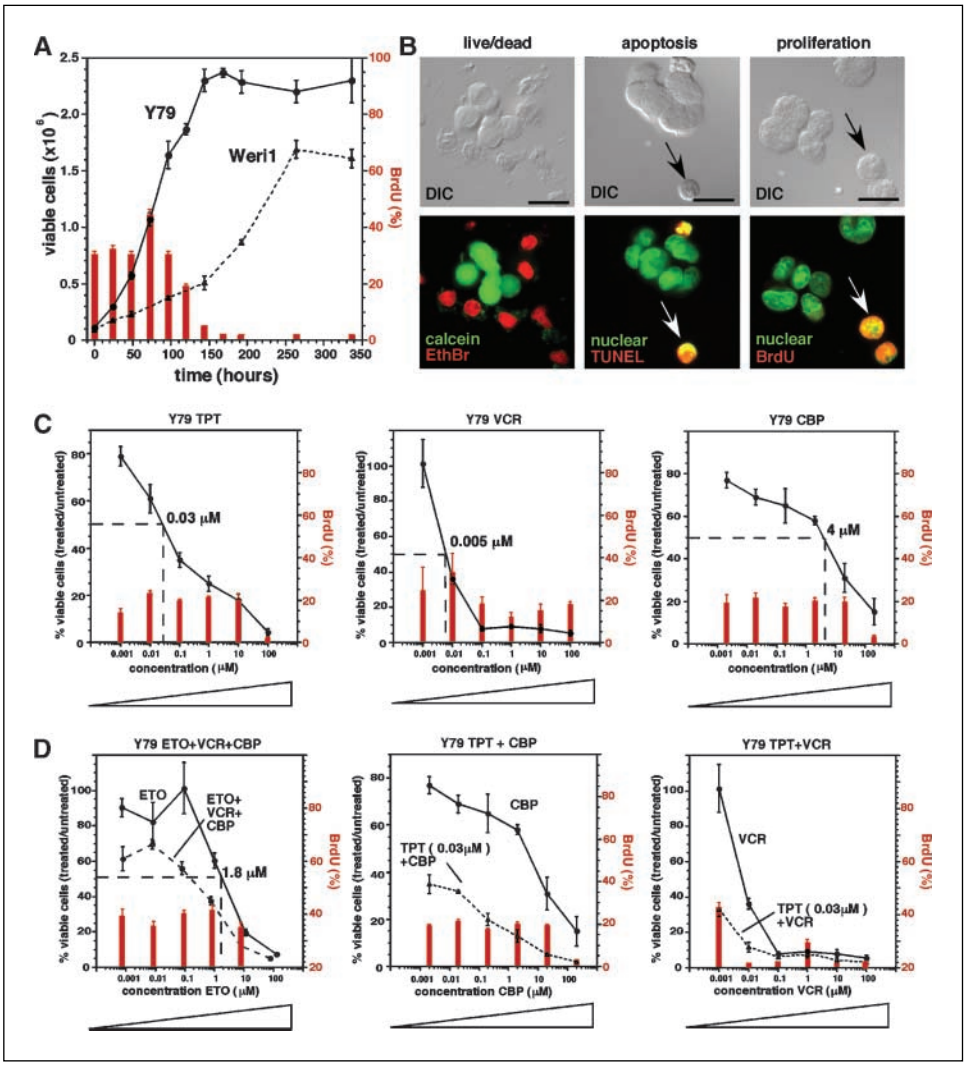

Fig. 1. Exposure of retinoblastoma cells to topotecan, vincristine, carboplatin, and etoposide in culture. *A,* Y79 and Weri1 retinoblastoma cell growth properties in RPMI were monitored to determine their optimum growth density. *B,* cell number, cell viability [calcein/ethidium bromide (*EthBr*)], and apoptosis (TUNEL) was used to calculate (see Materials and Methods) the viable cell number at each time point. The proportion of BrdU (*BrdU*) – labeled cells representative of the percentage of proliferating cells was determined separately (*red bars*). Bars, 10 μm. *C,* Y79 cells were exposed to different concentrations of topotecan (*TPT*), vincristine (*VCR*), or carboplatin (*CBP*) for 8 hours. Seventy-two hours later, the cell number and proportion of metabolically active cells (calcein/ethidium bromide), apoptotic cells (TUNEL), and dividing cells (BrdUrd) were scored and plotted. The concentration required to reduce cell viability by 50% (LC_{50}) is indicated by a *dashed line. D,* vincristine (0.005 μmol/L; *VCR*) and carboplatin (4 μmol/L) were combined with a broad range of etoposide (*ETO*) concentrations (*dashed line*), and viability was determined for Y79 (shown) and Weri1 cells. For comparison, a parallel experiment was carried out with etoposide alone (*solid line*). Topotecan (0.03 μmol/L) was combined with different concentrations of carboplatin or vincristine concentrations (*dashed line*), and viability was determined. For comparison, a parallel experiment was carried out with carboplatin or vincristine treatment alone (*solid line*). Points represent duplicate experiments done in triplicate.

revealed that the effects on cell cycle arrest were consistent with the fast-acting properties of topotecan and carboplatin as well as the slower-acting vincristine and etoposide (Fig. 2B). These cell cycle distribution analyses are also consistent with the mechanism of action for each drug. Topotecan and etoposide treatment leads to G_2 arrest, whereas carboplatin leads to G_2 arrest accompanied by an increase in S-phase cells. Vincristine treatment uncouples cell cycle progression from nuclear division resulting in the accumulation of cells with twice (8N) their normal DNA content (Fig. 2B).

Ocular pharmacokinetics of topotecan, vincristine, carboplatin, and etoposide. Although topotecan has a LC_{50} that is ~60-fold better than etoposide (0.03 μmol/L for topotecan and 1.8 μmol/L for etoposide), and a much shorter minimum time of exposure to achieve maximum reduction in cell viability (15 minutes for topotecan and 360 minutes for etoposide) if it does not efficiently penetrate the eye, it will not be a suitable replacement for etoposide in combination chemotherapy. Indeed, one of the primary hurdles for chemotherapeutic treatment of retinoblastoma is drug penetration through the blood-ocular barrier, which is made up of the zonulae occludens or tight junctions of the pigment epithelium and retinal capillaries into the vitreous (34). This is of particular importance, because vitreal seeds represent a primary clinical feature of late-stage bilateral retinoblastoma, and these small clusters of cells cannot be treated effectively with laser therapy or cryotherapy (1, 7).

To measure retinal and vitreal penetration of topotecan, carboplatin, vincristine, and etoposide, we injected each drug i.v. into 2-week-old rats; this age corresponded to the stage of treatment in our xenograft model. Drug levels were measured in the vitreous, retina, and plasma at 3 minutes, 30 minutes, 1.5 hours, 4 hours, and 6 hours after injection. A substantial amount of topotecan penetrated the vitreous as indicated by the area under the curve (AUC) vitreous/plasma ratio of 0.38 and retina/plasma ratio of 0.7 (Fig. 3A; data not shown). Carboplatin also had good vitreal penetration (AUC vitreous/plasma = 0.59), but only a low level of carboplatin was present in the retina (AUC retina/plasma = 0.03; Fig. 3B; data not shown). Etoposide penetrated the blood-ocular barrier with lower efficiency (AUC vitreous/plasma = 0.07; Fig. 3C) similar to that seen for the cerebrospinal fluid (35). Vincristine exhibited good vitreal and retinal penetration (AUC vitreous/plasma = 1.1; AUC retina/plasma = 1.0; Fig. 3D).

Response of retinoblastoma orthotopic xenografts to topotecan combination chemotherapy. To test the efficacy of topotecan combination chemotherapy for the treatment of retinoblastoma in the developing eye, we characterized an orthotopic retinoblastoma xenograft model using Y79 cells. Specifically, 1,000 cells were transplanted into the vitreous of newborn rats to approximate the stage of tumor formation in humans (ref. 36; Fig. 4A). Immunosuppression was not required in these animals, because rats are immunonaive for the first 24 hours after birth. For some experiments, the retinoblastoma cells were labeled with a GFP transgene to unambiguously establish tumor boundaries (Fig. 4A). Within 2 weeks, the engrafted cells proliferated, filled the vitreous, and reorganized the retinal vasculature (Fig. 4A; data not shown).

To establish a baseline before chemotherapy treatment in our retinoblastoma xenograft model, we analyzed cell number, survival, proliferation, apoptosis, and gene expression 2 weeks after engraftment. One hour before analysis, the rats received an i.p. injection of BrdU to label the cells in the S phase of the cell cycle, a measure of the fraction of dividing cells. The engrafted cells were microdissected from the normal tissue and dissociated; the total cell number was then scored. Calcein and ethidium bromide were used to measure metabolically active cells and dead cells, respectively (see Fig. 1 for an example). Eighty-five percent to 95% of Y79 cells were metabolically active after 2 weeks in the intraocular environment. The fraction of dividing cells was estimated by staining with an anti-BrdU antibody and scoring the fraction of immunopositive cells. Eight percent to 10% of Y79 tumor cells incorporated BrdU. To estimate the proportion of cells that had initiated apoptosis, we did a TUNEL assay. Two percent to 3% of cells had initiated apoptosis using the TUNEL assay. Fluorescent-activated cell sorting analysis showed that 52.6% were in G_0-G_1, 40.2% in S, and 7.2% in G_2-M (data not shown). The ratio of tumor to retinal volume (0.47 $\pm$ 0.21) was determined by removing the eye and reconstructing serial sections (Fig. 4B; data not shown).

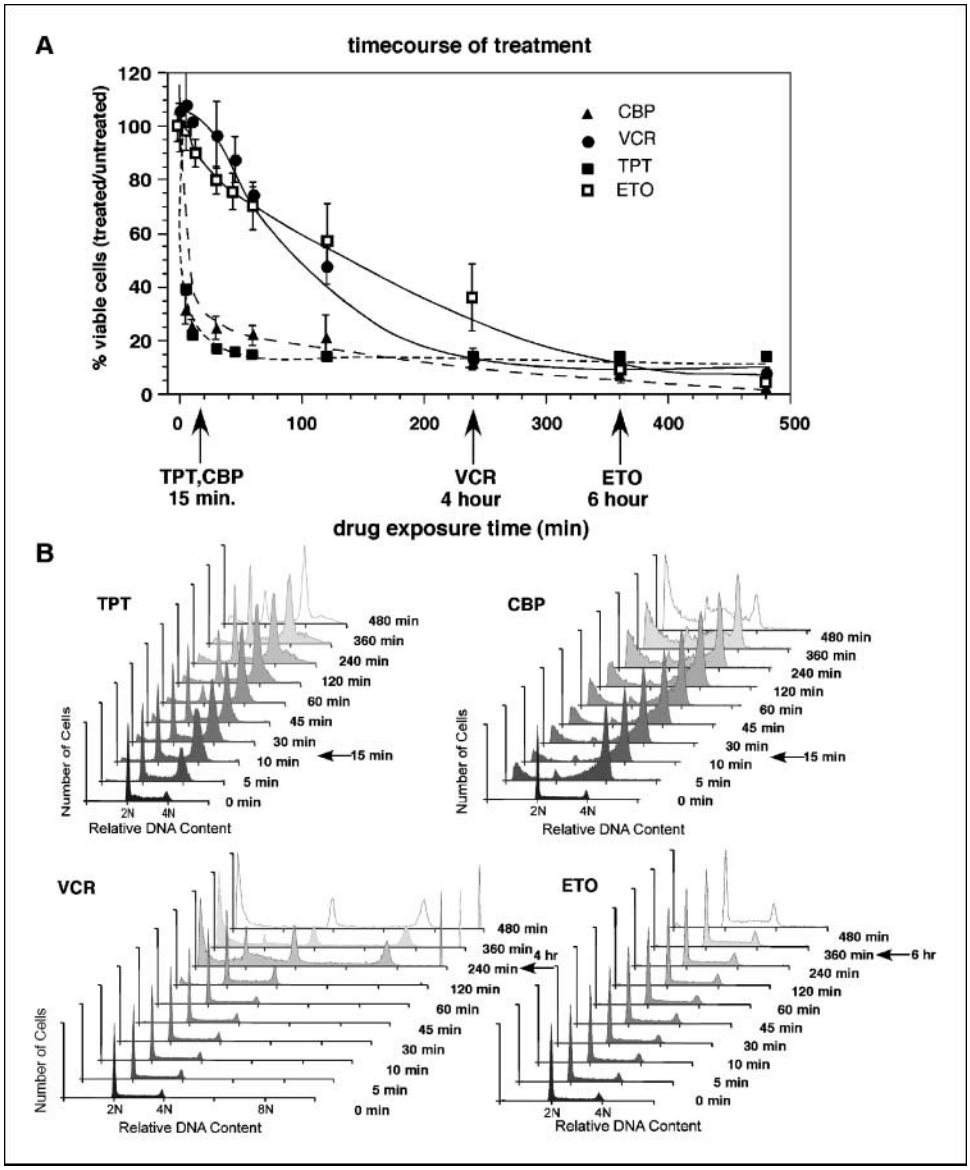

Fig. 2. Time of exposure analysis for topotecan, etoposide, carboplatin, and vincristine. *A,* Y79 cells were exposed to the LC_{50} of each drug (0.005 μmol/L vincristine or 0.03 μmol/L topotecan or 4 μmol/L carboplatin or 1.8 μmol/L etoposide) for different amounts of time. Following drug exposure, the samples were washed and cultured for 72 hours. *Arrows,* time required to achieve maximum reduction in cell viability. *Points,* mean of triplicate samples. *B,* DNA content of the samples plotted in (*A*) was determined by propidium iodide followed by fluorescent-activated cell sorting analysis.

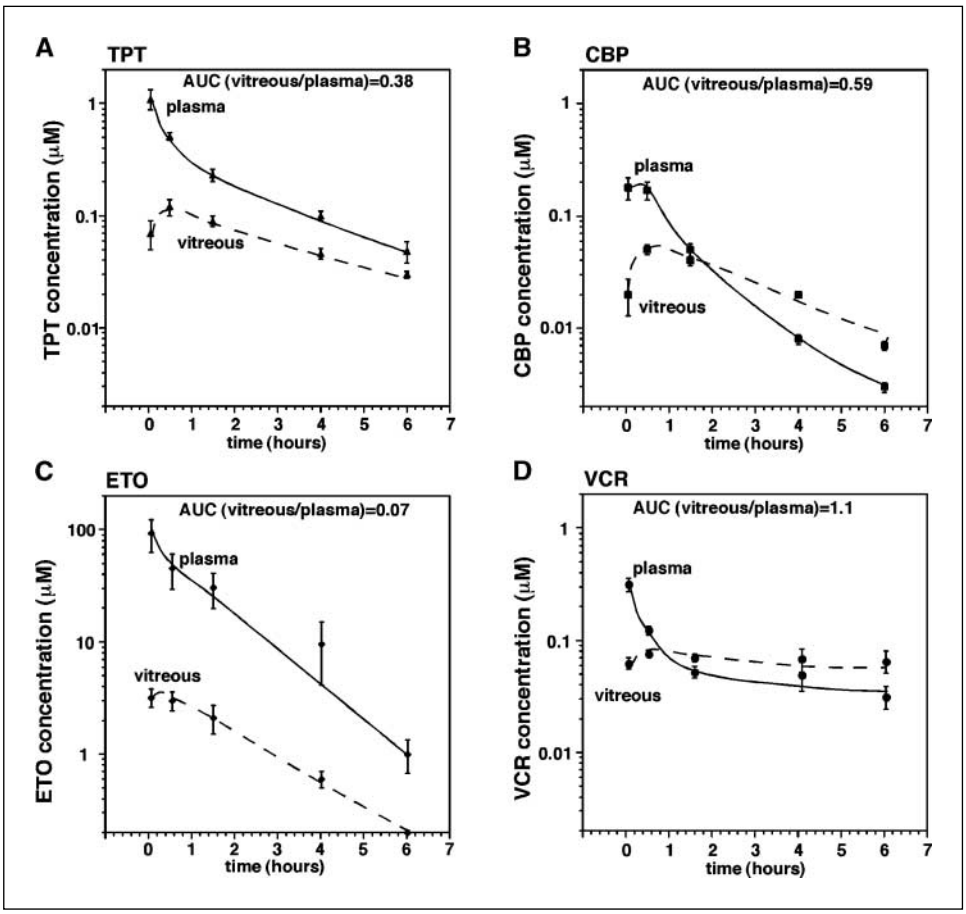

Fig. 3. Ocular pharmacokinetic analysis of topotecan, carboplatin, vincristine, and etoposide. *A-D,* pharmacokinetic analysis of topotecan, carboplatin, etoposide, and vincristine was carried out following tail vein injection to 2-week-old rats at the MTD for each drug. Plasma, vitreous, and retinae (data not shown) were isolated at each time point (3 minutes, 30 minutes, 1.5 hours, 4 hours, and 6 hours) and the concentration of topotecan (*A*), carboplatin (*B*), etoposide (*C*), and vincristine (*D*) was determined. Three animals were used for each time point in duplicate experiments. Data were fit to a two-compartment model and the AUC was calculated.

Having established a baseline, we tested each chemotherapeutic drug individually followed by topotecan combination chemotherapy. The two chemotherapeutic protocols that are currently being used for the treatment of children with retinoblastoma (etoposide + carboplatin + vincristine triple therapy and vincristine + carboplatin double therapy) were used as benchmarks for comparison with the topotecan combination chemotherapy. After one course of treatment, the transplanted retinoblastoma cells were analyzed for viability and proliferation as described above (Fig. 4A). Carboplatin was the most effective single drug in this assay reducing the cell number/eye from $2.4 \pm 0.6 \times 10^6$ to $0.79 \pm 0.29 \times 10^6$ ($P < 0.0001$). Topotecan combined with carboplatin was the most potent combination therapy, reducing cell number further to $0.22 \pm 0.11 \times 10^6$ ($P < 0.001$). Vincristine showed little effect on retinoblastoma cell survival in our xenograft model using this short-term assay (Fig. 4A). Similarly, when vincristine was combined with topotecan (Fig. 4A) or carboplatin (data not shown), there was very little additional reduction in cell number beyond carboplatin or topotecan alone. Importantly, the combination of topotecan with carboplatin reduced the number of viable cells ($0.22 \pm 0.11 \times 10^6$ cells per eye) in this model more effectively than the triple drug therapy ($2.02 \pm 1.08 \times 10^6$; $P < 0.001$) or the combination of etoposide and carboplatin ($1.88 \pm 1.05 \times 10^6$; $P < 0.001$; Fig. 4A). Three-dimensional reconstruction of the tumor and retina confirmed that the tumor volume in addition to the proportion of viable tumor cells was reduced following chemotherapy treatment (Fig. 4B).

It was possible that there was a minor effect of vincristine treatment that was masked in our system by the active proliferation and expansion of the xenograft. One of the hallmarks of vincristine exposure is a nucleus with twice the genomic DNA content (see Fig. 2B), because vincristine blocks cytokinesis without halting cell cycle progression. To test if there was any vincristine-mediated block of mitosis, we scored the proportion of large cells with twice the genomic DNA content in cultured cells and xenografts following vincristine treatment (Fig. 4C). Ninety-eight percent of cells treated with 5 nmol/L vincristine for 8 hours in culture exhibited twice their normal DNA content; $2 \pm 1\%$ of xenografts treated with vincristine exhibited morphologic features consistent with continued cell cycle progression without cytokinesis. The proportion of enlarged nuclei in xenografts was similar to control xenografts ($3 \pm 2\%$), consistent with the lack of a robust vincristine response in the intraocular environment.

To analyze the response of individual tumor xenografts over time in the same animal, we took advantage of a Y79 cell line (Y79-LUC) constitutively expressing the luciferase gene (a generous gift of Dr. Andrew Davidoff; Fig. 4D). Using the Xenogen imaging system, rats with a Y79-LUC orthotopic xenograft were analyzed daily from P7 to P28 to monitor tumor growth and tumor response following topotecan + carboplatin administration. Luciferase intensity was found to correlate with tumor volume and tumor cell number (data not shown). These data show that there is a rapid reduction in tumor cell number following topotecan + carboplatin treatment (Fig. 4D).

Response of focal mouse retinal tumors to topotecan combination chemotherapy. Having shown that the combination of topotecan and carboplatin was the most effective short-term treatment of retinoblastoma xenografts, we then tested the efficacy of each drug and drug combination by treating mice that had a few focal, clonal retinal tumors. We injected the LIA-E^{E1A} retrovirus encoding the 13S *E1A* oncogene and an alkaline phosphatase reporter gene into the subretinal space of newborn $p53^{-/-}$ mice at a titer sufficient to achieve one to five clones per retina (37). Within 3 weeks, infected retinal progenitor cells proliferated, spread laterally through the retinal vasculature (Fig. 5A), and eventually filled the entire eye (Fig. 5B). Newborn $p53^{-/-}$ mice were injected with the LIA-E^{E1A} retrovirus, and at 6 weeks of age, they received chemotherapeutic treatment (topotecan, carboplatin, vincristine, etoposide, topotecan + vincristine, etoposide + carboplatin, and topotecan + carboplatin) for 8 weeks (Fig. 5C and D) in groups of 14 to 16 animals. Following treatment, retinae were removed, dissociated, and stained for alkaline phosphatase expression, and the proportion of tumor cells was scored (Fig. 5C and D). The dose and schedule of treatment were consistent with that used for the treatment of children with retinoblastoma or other brain tumors (see Materials and Methods). As in the xenograft studies, the combination of topotecan and carboplatin was more effective than either drug alone (Fig. 5D). Moreover, no additional antitumor effect was seen by combining topotecan with vincristine (Fig. 5D) compared with topotecan alone. The combination of topotecan + carboplatin was more effective than etoposide + carboplatin in this assay ($P < 0.01$; Fig. 5D).

Discussion

We have developed two new rodent models of retinoblastoma that emphasize the initiation of disease during development and focal, clonal tumor formation. Both models were used to test topotecan combination chemotherapy to determine if this may be an alternative to current triple drug therapy using etoposide/vincristine/carboplatin for the treatment of retinoblastoma. Consistent with clinical trials using topotecan

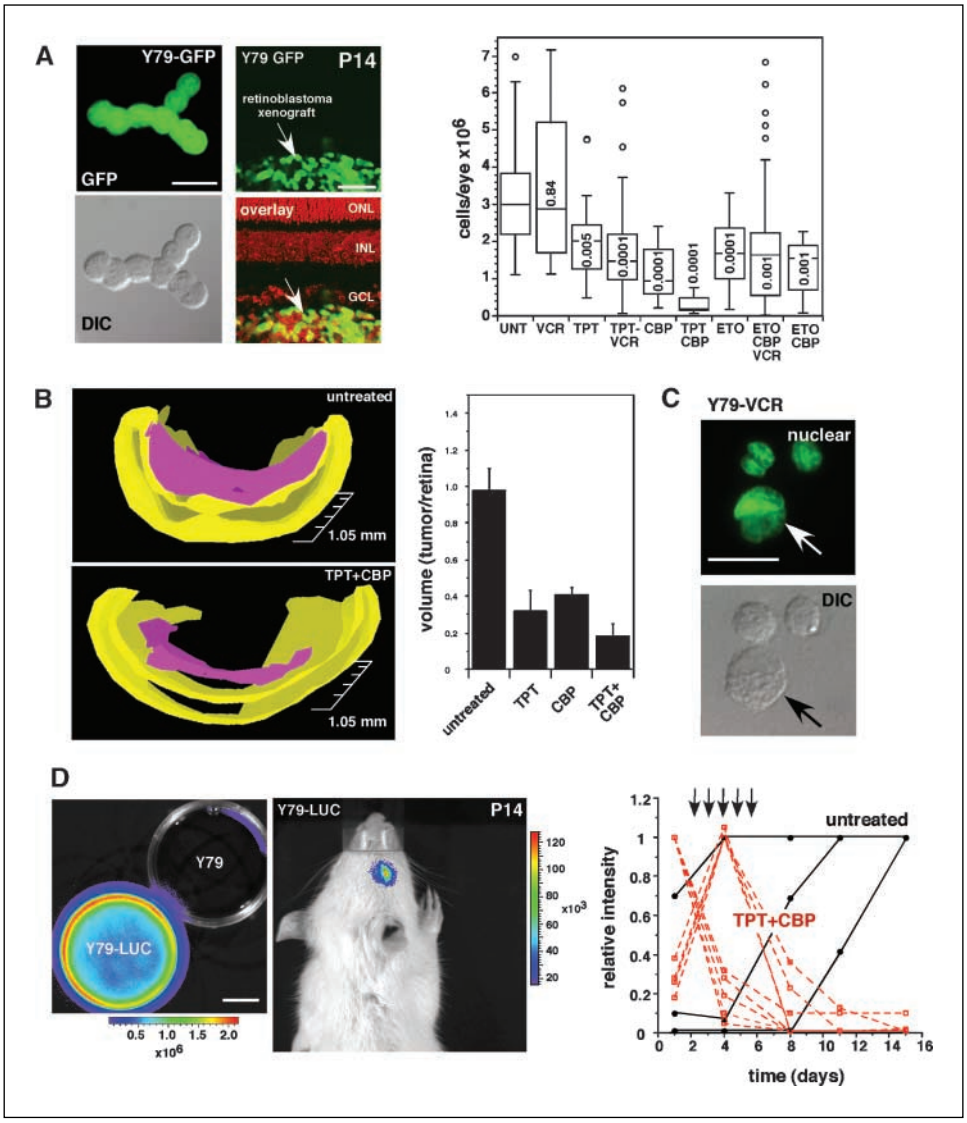

Fig. 4. A developmentally appropriate orthotopic retinoblastoma xenograft model. *A,* Y79 retinoblastoma cells were labeled with GFP by stably transfecting a GFP-expressing plasmid. A total of 1,000 cells in a volume of 1 μL were injected into the vitreous of newborn rats. Using the GFP-labeled Y79 cells, the tumor boundary (*green*) can be clearly distinguished from the counterstained nuclei (*red*). After 2 weeks, the cells had proliferated and filled the vitreous (*arrow*). Two-week-old rats with retinoblastoma xenografts (~ 25 animals per group) were treated with one MTD of each drug or combination. One week after treatment, the number of viable cells was calculated in the same manner as for cultured cells exposed to these drugs. The mean, SD, and *P*s are shown for each treatment compared with untreated tumor. Twenty-five to 30 animals were used for each experiment. Bars, 10 μm for single cells and 50 μm for tissue sections. *B,* in a parallel experiment, the tumor volume following chemotherapeutic treatment was calculated by reconstructing serial sections into a three-dimensional representation. *Yellow,* retina; *pink,* tumor. Representative three-dimensional reconstructions are shown for untreated and topotecan + carboplatin treated xenografts. The tumor to retinal volume ratio data from six to eight animals per group is plotted. *C,* retinoblastoma cells treated with vincristine in culture continue to replicate their DNA (*green*) without undergoing cytokinesis resulting in nuclei with twice the normal amounts of genomic DNA (*arrow*). *D,* Y79-LUC cells exposed to Luciferin and imaged with the Xenogen imaging system. A P14 rat is shown that received 1,000 Y79-LUC intravitreal injection at P0. Data are plotted for a representative of eight rats exposed to topotecan + carboplatin compared with control animals (*red dashed lines*). *Arrows,* days of chemotherapy administration. Rats received the clinically relevant dose of 0.1 mg/kg topotecan daily ×5 followed by one dose of carboplatin (18 mg/kg). Abbreviations: *ONL,* outer nuclear layer; *INL,* inner nuclear layer; *GCL,* ganglion cell layer.

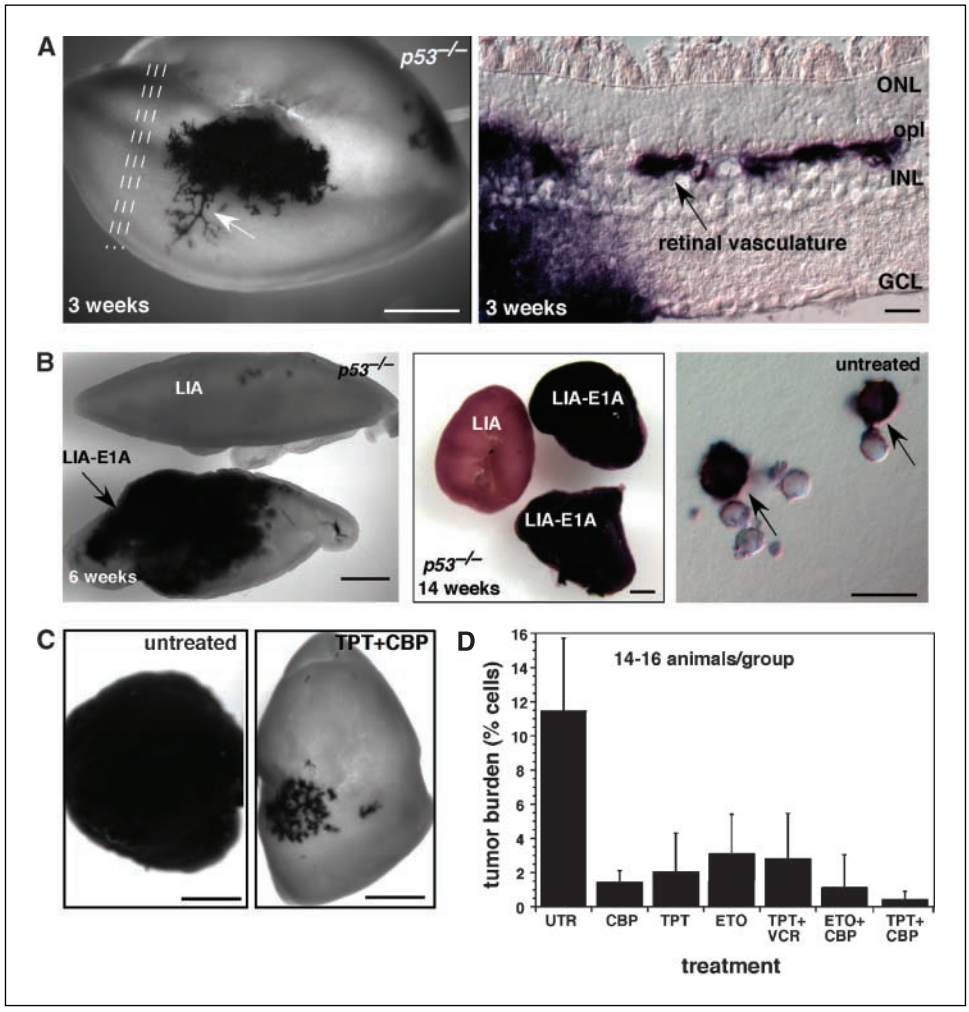

Fig. 5. Response of focal, clonal retinoblastoma to chemotherapy. *A,* injection of a replication incompetent retrovirus (LIA-E^{E1A}) into the eyes of newborn $p53^{-/-}$ mice leads to hyperproliferation of retinal progenitor cells by 3 weeks of age. This retrovirus encodes the E1A 13S oncogene and the alkaline phosphatase reporter gene. *Dashed lines,* plane of sections shown in the adjacent panel. *Arrow,* lateral spread of retinoblastoma cells through the retinal vasculature. Cross-section showing invasion of the retinal cells expressing E1A into the retinal vasculature at the outer plexiform layer (*opl*). *B,* by 6 weeks of age, the hyperplasia has spread across much of the retinal volume. The control retrovirus (LIA-E^{E1A}) injected into the contralateral eye of the same animal does not exhibit this hyperproliferative clonal phenotype. By 14 weeks, the entire ocular space is often filled with alkaline phosphatase – expressing tumor cells. The proportion of alkaline phosphatase – positive cells can be determined by dissociating the retina, plating the cells on glass slides and staining for alkaline phosphatase expression. *C, D,* treatment of these clonal, focal tumors resulted in a reduction in the size of the tumors and a reduction in the proportion of alkaline phosphatase – labeled cells. The relative proportion of alkaline phosphatase – expressing cells was calculated for each retina and averaged. Bars, 1 mm for whole retinae (*A-C*); 25 μm (*A*, transverse section); 10 μm (*B*, dissociated cells).

(38–40), we found that this topoisomerase I inhibitor was effective for the treatment of retinoblastoma in our preclinical models. Our preclinical studies also showed that the combination of topotecan and carboplatin was more effective than topotecan + vincristine, etoposide + carboplatin, or etoposide + carboplatin + vincristine. Importantly, we found that vincristine exhibited little efficacy for the treatment of retinoblastoma alone or in combination. Taken together, these data suggest that topotecan + carboplatin may be an effective alternative to triple drug therapy (etoposide/carboplatin/vincristine) for the treatment of children with retinoblastoma. In addition, using a combination of cell culture, ocular pharmacokinetics, and rodent models, we can now efficiently test new chemotherapeutic drug combinations, doses, and schedules to identify treatment approaches that may improve the ocular salvage rate for children with bilateral retinoblastoma.

Two new preclinical models of retinoblastoma. Most animal models have inherent strengths and weaknesses (1); thus, we have combined two complementary models of retinoblastoma to test topotecan combination chemotherapy. By injecting a few human retinoblastoma cells (1,000 cells) into the vitreous of newborn rats, we overcame the need to use immunocompromised animals (11). In addition, this orthotopic model more faithfully recapitulates the human disease, because the transplanted cells grow in a developmental environment similar to that of the human retinal tumors (41). The developmental stage is important, because the differences between the fetal eye and the adult eye in terms of the growth factors that are expressed, retinal vasculature, and cytoarchitecture may affect retinoblastoma formation (discussed in ref. 41). Our retroviral model of retinoblastoma also relies on the appropriate developmental stage of tumor initiation. Importantly, by injecting LIA-E^{E1A} into the eyes of newborn $p53^{-/-}$ mice, we have created focal, clonal retinoblastoma. In the short-term studies described in this article (5 weeks for rats and 14 weeks for mice), we did not detect any metastatic retinoblastoma. Data from additional long-term studies (up to 8 months) have revealed that there is some invasion into the optic nerve and anterior chamber. However, these tumors rapidly lead to ocular rupture, requiring euthanasia and making them useless as a model for metastatic retinoblastoma. Studies are under way using primary human and mouse retinoblastoma cells in immunocompromised mice to recapitulate some of the features of metastatic retinoblastoma.

One of the major advantages of these two new preclinical models of retinoblastoma is that they are relatively high throughput in comparison with our newly developed knockout model of retinoblastoma (14). Therefore, we will use the cell

culture studies combined with pharmacokinetics and our xenograft and retroviral models as an initial screen of new therapies. The most promising chemotherapeutic combinations will then be tested in our retinoblastoma knockout mouse model before incorporation into clinical trials. Future efforts will focus on comparing topotecan + carboplatin to triple drug therapy in the retinoblastoma knockout mouse model (14).

Poor efficacy of vincristine for the treatment of retinoblastoma. Vincristine most effectively killed retinoblastoma cells in culture and penetrated the blood-ocular barrier; however, vincristine required a relatively long exposure time (4 hours) to kill retinoblastoma cells in culture. Although the pharmacokinetics suggest that there was a high enough concentration of vincristine in the vitreous for a period of time sufficient to kill the retinoblastoma cells, it was not effective in our preclinical models alone, nor did vincristine provide any additional benefit when combined with topotecan or carboplatin. There are several possible explanations for this result. First, vincristine may be bound to proteins in the vitreous and cannot efficiently penetrate the tumor. Second, it is possible that vincristine is degraded or modified (42), rendering it ineffective against the retinoblastoma cells. The relatively long time of exposure required for vincristine may exacerbate this effect. The quantitation of vincristine in the vitreous was based on the counts detected from the [^{3}H]vincristine. Therefore, our assay cannot distinguish between a processed, degraded, or protein-bound form of vincristine. Other methods of detecting the intact molecule of vincristine could not be used for these samples because the volume (20 μL) of vitreous obtained from 2-week-old rats is too small. Additional pharmacokinetic studies in larger mammals, such as rabbits, will be necessary to determine why vincristine was not effective for the treatment of retinoblastoma in preclinical rodent models. It is not known how effective vincristine is at halting retinoblastoma progression in humans, because clinical trials with vincristine alone have not been carried out, only combination therapy.

Ocular pharmacokinetics. Vitreal seeds are one of the biggest clinical challenges of treating late-stage bilateral retinoblastoma. These small clusters of 50 to 1,000 tumor cells are a challenge, because individual seeds can settle near the retinal vasculature, begin to divide, and form new tumor foci after treatment. While in the vitreous, seeds are difficult to treat with laser therapy or cryoablation, making chemotherapy the primary mode of treatment for retinoblastoma with extensive vitreal seeding. Ocular pharmacokinetics studies are essential to determine if chemotherapeutic drugs penetrate the vitreous. However, even when a drug, such as vincristine, penetrates the vitreous efficiently, it does not guarantee that it will be an effective treatment for retinoblastoma. Other factors, such as drug stability or modifications, may also influence efficacy in preclinical models (42).

Clinical trials using topotecan combination chemotherapy. Based on our cell culture studies, ocular pharmacokinetic experiments, and analysis of preclinical models, we have found that the combination of topotecan with carboplatin may be an effective alternative to the triple drug therapy (etoposide/carboplatin/vincristine) that is currently used to treat retinoblastoma. The advantage of topotecan combined with carboplatin is that it is more effective in our preclinical models compared with etoposide + carboplatin or etoposide + carboplatin + vincristine. In addition, there are no secondary malignancies associated with topotecan exposure as has been reported for etoposide (8). However, this does not mean that systemic topotecan exposure is not associated with significant side effects. Some of the most severe include myelosuppression and general hematotoxicity (38–40). It is even more difficult to manage the side effects of systemic topotecan and carboplatin exposure. In a study of topotecan and carboplatin in patients with solid tumors, it was found that, at a constant systemic exposure of carboplatin, hematotoxicity was the major obstacle to topotecan dose escalation (43).

One way to minimize such toxicity is to adjust the dose, schedule, and site of administration of the drugs. A recent study using a transgenic mouse model of retinoblastoma found that subconjunctival carboplatin administration was effective at reducing tumor size (44). Another study of patients with retinoblastoma found that low-dose, frequent administration of topotecan more effectively reduced the tumor burden than did infrequent, high-dose administration of topotecan (45). Therefore, it will be interesting to test the combination of frequent, low-dose topotecan given with subconjunctival carboplatin. This regimen may reduce secondary toxicity while retaining effective vitreal and retinal penetration.

Acknowledgments

We thank K. Eder, K. Balbi, C. Brannon, and S. Culpepper for assistance with cell culture work, Drs. C. Rodriguez-Galindo and M. Wilson for helpful discussions, Dr. Andrew Davidoff for providing the Y79-LUC cell line, and A. McArthur for editing the article.

References

1. Dyer MA. Mouse models of childhood cancer of the nervous system. J Clin Pathol 2004;57:561–76.
2. Young J, Smith M, Roffers S, Liff J, Bunin G. Retinoblastoma. Bethesda: National Cancer Institute; 2003.
3. Gurney J, Smith M, Ross J. Cancer among infants. Bethesda: National Cancer Institute; 2003.
4. DiCiommo D, Gallie BL, Bremner R. Retinoblastoma: the disease, gene and protein provide critical leads to understand cancer. Semin Cancer Biol 2000;10:255–69.
5. Knudson A, Strong L. Mutations and cancer: neuroblastoma and pheochromocytomea. Am J Hum Genet 1972;24:514–22.
6. Rodriguez-Galindo C, Wilson MW, Haik BG, et al. Treatment of metastatic retinoblastoma. Ophthalmology 2003;110:1237–40.
7. Rodriguez-Galindo C, Wilson MW, Haik BG, et al. Treatment of intraocular retinoblastoma with vincristine and carboplatin. J Clin Oncol 2003;21:2019–25.
8. Nishimura S, Sato T, Ueda H, Ueda K. Acute myeloblastic leukemia as a second malignancy in a patient with hereditary retinoblastoma. J Clin Oncol 2001;19:4182–3.
9. Romer JT, Curran T. Medulloblastoma and retinoblastoma oncology recapitulates ontogeny. Cell Cycle 2004;3:917–9.
10. Romer JT, Kimura H, Magdaleno S, et al. Suppression of the Shh pathway using a small molecule inhibitor eliminates medulloblastoma in Ptc1+/−,p53−/− mice. Cancer Cell 2004;6:229–400.
11. del Cerro M, Seigel GM, Lazar E, et al. Transplantation of Y79 cells into rat eyes: an *in vivo* model of human retinoblastomas. Invest Ophthalmol Vis Sci 1993;34:3336–46.
12. Chevez-Barrios P, Hurwitz MY, Louie K, et al. Metastatic and nonmetastatic models of retinoblastoma. Am J Pathol 2000;157:1405–12.
13. O'Brien JM, Marcus DM, Bernards R, et al. A transgenic mouse model for trilateral retinoblastoma. Arch Ophthalmol 1990;108:1145–51.
14. Zhang J, Schweers B, Dyer MA. The first knockout

mouse model of retinoblastoma. Cell Cycle 2004;3:952–9.

15. Chen D, Livne-Bar I, Vanderluit JL, Slack RS, Agochiya M, Bremner R. Cell-specific effects of RB or RB/p107 loss on retinal development implicate an intrinsically death-resistant cell-of-origin in retinoblastoma. Cancer Cell 2004;5:539–51.

16. MacPherson D, Sage J, Kim T, Ho D, McLaughlin ME, Jacks T. Cell type-specific effects of Rb deletion in the murine retina. Genes Dev 2004;18:1681–94.

17. Thompson J, Stewart CF, Houghton PJ. Animal models for studying the action of topoisomerase I targeted drugs. Biochim Biophys Acta 1998;1400:301–19.

18. Thompson J, George EO, Poquette CA, et al. Synergy of topotecan in combination with vincristine for treatment of pediatric solid tumor xenografts. Clin Cancer Res 1999;5:3617–31.

19. Houghton JA, Cook RL, Lutz PJ, Houghton PJ. Childhood rhabdomyosarcoma xenografts: responses to DNA-interacting agents and agents used in current clinical therapy. Eur J Cancer Clin Oncol 1984;20:955–60.

20. Houghton JA, Williams LG, Torrance PM, Houghton PJ. Determinants of intrinsic sensitivity to *Vinca* alkaloids in xenografts of pediatric rhabdomyosarcomas. Cancer Res 1984;44:582–90.

21. Gaynon PS, Ettinger LJ, Baum ES, Siegel SE, Krailo MD, Hammond GD. Carboplatin in childhood brain tumors. A Children's Cancer Study Group phase II trial. Cancer 1990;66:2465–9.

22. Allen JC, Walker R, Luks E, Jennings M, Barfoot S, Tan C. Carboplatin and recurrent childhood brain tumors. J Clin Oncol 1987;5:459–63.

23. McFall RC, Sery TW, Makadon M. Characterization of a new continuous cell line derived from a human retinoblastoma. Cancer Res 1977;37:1003–10.

24. Dyer MA, Cepko CL. p27Kip1 and p57Kip2 regulate proliferation in distinct retinal progenitor cell populations. J Neurosci 2001;21:4259–71.

25. Zhu CC, Dyer MA, Uchikawa M, Kondoh H, Lagutin OV, Oliver G. Six-3 mediated auto repression and eye development requires its interaction with members of the Grouch-related family of co-repressors. Development 2002;129:2835–49.

26. Dyer MA, Cepko CL. p57(Kip2) regulates progenitor cell proliferation and amacrine interneuron development in the mouse retina. Development 2000;127:3593–605.

27. Simpson AE, Gilbert JA, Rudnick DE, Geroski DH, Aaberg TM, Jr., Edelhauser HF. Transscleral diffusion of carboplatin: an *in vitro* and *in vivo* study. Arch Ophthalmol 2002;120:1069–74.

28. Cai X, Woo MH, Edick MJ, Relling MV. Simultaneous quantitation of etoposide and its catechol metabolite in human plasma using high-performance liquid chromatography with electrochemical detection. J Chromatogr 1999;728:241–50.

29. Schouten-Van Meeteren AY, Moll AC, Imhof SM, Veerman AJ. Overview: chemotherapy for retinoblastoma: an expanding area of clinical research. Med Pediatr Oncol 2002;38:428–38.

30. Dyer MA. Regulation of proliferation, cell fate specification and differentiation by the homeodomain proteins Prox1, Six3, and Chx10 in the developing retina. Cell Cycle 2003;2:350–7.

31. Dyer MA, Cepko CL. The p57(Kip2) cyclin kinase inhibitor is expressed by a restricted set of amacrine cells in the rodent retina. J Comp Neurol 2001;429:601–14.

32. Wang LG, Liu XM, Kreis W, Budman DR. The effect of antimicrotubule agents on signal transduction pathways of apoptosis: a review. Cancer Chemother Pharmacol 1999;44:355–61.

33. Tonda ME, Murry DJ, Rodman JH. Formation of platinum-DNA adducts in pediatric patients receiving carboplatin. Pharmacotherapy 1996;16:631–7.

34. Peyman GA, Schulman JA. Intravitreal drug therapy. Jpn J Ophthalmol 1989;33:392–404.

35. Relling MV, Mahmoud HH, Pui CH, et al. Etoposide achieves potentially cytotoxic concentrations in CSF of children with acute lymphoblastic leukemia. J Clin Oncol 1996;14:399–404.

36. Clancy B, Darlington RB, Finlay BL. Translating developmental time across mammalian species. Neuroscience 2001;105:7–17.

37. Zhang J, Gray J, Wu L, et al. Rb regulates proliferation and rod photoreceptor development in the mouse retina. Nat Genet 2004;36:351–60.

38. Chantada GL, Fandino AC, Casak SJ, Mato G, Manzitti J, Schvartzman E. Activity of topotecan in retinoblastoma. Ophthalmic Genet 2004;25:37–43.

39. Frangoul H, Ames MM, Mosher RB, et al. Phase I study of topotecan administered as a 21-day continuous infusion in children with recurrent solid tumors: a report from the Children's Cancer Group. Clin Cancer Res 1999;5:3956–62.

40. Nitschke R, Parkhurst J, Sullivan J, Harris MB, Bernstein M, Pratt C. Topotecan in pediatric patients with recurrent and progressive solid tumors: a Pediatric Oncology Group phase II study. J Pediatr Hematol Oncol 1998;20:315–8.

41. Dyer MA, Bremner R. The search for the retinoblastoma cell of origin. Nat Rev Cancer 2005;5:91–101.

42. Houghton JA, Williams LG, Houghton PJ. Stability of vincristine complexes in cytosols derived from xenografts of human rhabdomyosarcoma and normal tissues of the mouse. Cancer Res 1985;45:3761–7.

43. Athale UH, Stewart C, Kuttesch JF, et al. Phase I study of combination topotecan and carboplatin in pediatric solid tumors. J Clin Oncol 2002;20:88–95.

44. Hayden BH, Murray TG, Scott IU, et al. Subconjunctival carboplatin in retinoblastoma: impact of tumor burden and dose schedule. Arch Ophthalmol 2000;118:1549–54.

45. Tubergen DG, Stewart CF, Pratt CB, et al. Phase I trial and pharmacokinetic (PK) and pharmacodynamics (PD) study of topotecan using a five-day course in children with refractory solid tumors: a pediatric oncology group study. J Pediatr Hematol Oncol 1996;18:352–61.